ASIAN JOURNAL OF CIVIL ENGINEERING (BUILDING AND HOUSING) VOL. 13, NO. 4 (2012)
PAGES 571-583

Technical Note

SEISMIC BEHAVIOUR OF EXTERIOR BEAM-COLUMN JOINTS WITH SQUARE SPIRAL CONFINEMENT

P. Asha[*a], R. Sundararajan[b]
[a]Larsen and Toubro Ltd., Chennai, Tamilnadu, India
[b]Government College of Technology, Coimbatore, Tamilnadu, India

Received: 10 Sepember 2010; **Accepted:** 30 October 2011

ABSTRACT

This paper presents the seismic behavior of exterior beam-column joints with square spiral confinement in the joint region along with different reinforcement detailing for anchorage of beam bars, confinement in joint and additional reinforcement in beam and column. The performance of the specimens are compared in terms of lateral load-displacement hysteresis loop, load ratio, percent of initial stiffness versus displacement curves, total energy dissipation, beam rotation at distances of D and 2D, strain in beam main bars and crack pattern. Among all, the specimen with inclined bars from beam to column (named as SS2) was the most effective considering all the parameters taken for comparison. It is concluded that inclined bars from column to beam in SS2 can successfully move the plastic hinge away from the column face.

Keywords: Joint; confinement; hysteresis; stiffness; energy; strain; detailing

1. INTRODUCTION

During a strong earthquake, beam-column joints are subjected to severe reversed cyclic loading. They constitute one of the critical regions and they must be designed and detailed to dissipate large amounts of energy without loss of strength and stiffness. Consequently, the ductile behavior of reinforced concrete structures dominantly depends on the reinforcement detailing of the beam-column joints. Failure of the joint region can not only damage the column load paths but also adversely affect the ductility and energy dissipation capacity of the frame as whole. Murty et al [1] reported that many reinforced concrete buildings suffered severe damage and/or collapse in recent earthquakes due to poor detailing of joint reinforcement (amount of transverse shear reinforcement in joints and anchorage of

[*] E-mail address of the corresponding author: asha_panchanathan@yahoo.co.in (P. Asha)

longitudinal beam bars in columns).

The behaviour of beam-column joints under seismic loading has been studied by several researchers over the last five decades. The areas investigated varied from design procedures and joint details to analytical modeling of beam-column joints. Hanson and Connor [2] tested seven full size exterior beam column joints and observed that the presence of axial load on column improved the behaviour and stressed the importance of proper detailing of the joint. Ehsani and Wight [3] investigated the effect of key variables on the behaviour of external reinforced beam to column connection subjected to earthquake type loading. The primary variables were the ratio of the column to beam flexural capacity, the joint shear stresses and the transverse reinforcement in the joint. Their tests indicated that additional transverse reinforcement enhanced the behaviour of sub assemblage but the construction of such connection was found to be extremely difficult.

Tsonos et al [4] studied the improvement in the seismic behaviour of exterior reinforced concrete beam-column joints resulting from the presence of inclined reinforcing bars in the joint region. They concluded that exterior beam-column joints with crossed inclined bars showed high strength and large energy dissipation capacity.

Kumar et al [5] carried out an experimental study to clarify the effect of joint detailing on the seismic performance of lightly reinforced concrete frames. The parameters studied were the effect of joint rotation, column axial load, cross-reinforcement in the joint and percentage of longitudinal reinforcement in the beam. They found that use of cross reinforcement in the joint reduced damage in the joint but also reduced the ductility and energy dissipation capacity. The test results indicated that presence of axial load in column and allowing free joint rotation increased the strength and ductility but also reduced the damage in the joint region.

Murty et al [1] evaluated the effectiveness of different details of longitudinal beam bar anchorage and transverse joint reinforcement in exterior beam-column joints of moment resistant frames. They concluded that of all the joint reinforcement detailing schemes investigated, the ACI standard hook with hairclip-type transverse reinforcement was a preferred combination because of its ease of construction and overall effectiveness.

The emphasis of the present study is the evaluation of the seismic performance of exterior joints having square spiral confinement with different anchorage details of beam longitudinal reinforcement and joint transverse reinforcement. This study also aims to investigate the use of welded wire fabric for additional confinement of column and joint region subjected to cyclic loading and as additional shear reinforcement in plastic hinge zone of beam. An attempt has also been made to relocate the plastic hinge formation from face of column by means of different detailing techniques.

2. EXPERIMENTAL INVESTIGATION

2.1 Details of test specimens

The test specimens were 1/4 scale models of typical exterior beam-column joints made up of a single column with one beam in the longitudinal direction. All specimens were cut at mid-height of supporting column and at midspan of beams, which were the assumed points of

inflection. Figure 1 shows a sketch of test specimens with overall dimensions.

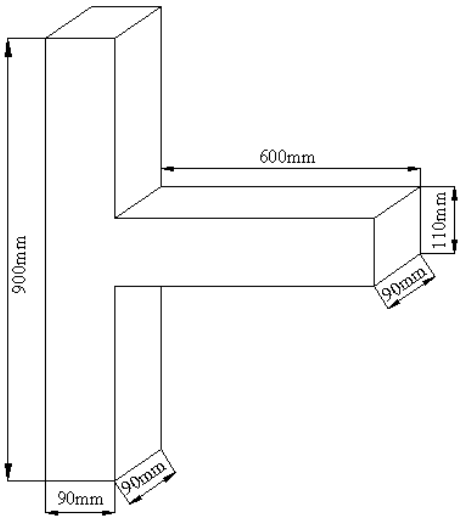

Figure 1. Overall dimensions of test specimens

The specimens were designed for gravity loads as per IS 456-2000 [6] and earthquake forces. The earthquake forces were calculated for Zone III as per IS 1893-(Part 1) 2002 [7]. The specimens were designed for seismic forces and detailed as per IS 13920-1993 [8]. The first specimen is SS (Figure 2) which had Square Spiral confinement in the joint which was extended into column. Five other reinforcement detailing schemes were incorporated in SS and the specimens are designated as SS1, SS2, SS3, SS4 and SS5 (Figure 3). Hence all the six specimens were having same dimensions and same shape of confinement (square spirals) with variance in the reinforcement detailing. The objective of this investigation is to improve the seismic performance of exterior beam-column joints through combined effect of square spiral confinement and five different types of reinforcement detailing.

SS1 indicates specimen having longitudinal beam bars with inclined anchorage and SS2 had four inclined bars that extend from column to beam, two from the column portion above the joint and two from the column portion below the joint. The specimen SS3 was provided with four supplementary bars in beam, two at top and two at bottom which were intersected to form 'X' shape. The beam main bars in SS3 were provided with round hook anchorage. SS4 had box-shaped welded wire mesh in the joint region alone as additional confinement whereas SS5 had welded wire mesh in column and beam as additional main and transverse reinforcement. The spacing of transverse reinforcement in joint and throughout in beam and column was maintained as D/2 in SS5 where 'D' is the overall depth of member. Welded wire mesh used was made up of 2.2mm diameter with spacing 25.4mm c/c. In SS1, SS2, SS3 and SS4 the joint and areas in beam upto a distance of 2D were provided with transverse reinforcement with D/4 spacing as that of SS as per recommendations of IS 13920-1993[8]. The transverse reinforcement in column was spaced at D/4 to a height of l_o (l_o is the length of member over which special confinement reinforcement is to be provided) above and below the level of joint in the column which was calculated as 180 mm according

to IS 13920[8]. The percentage of column, beam and joint reinforcement of the test specimens is given in Table 1.

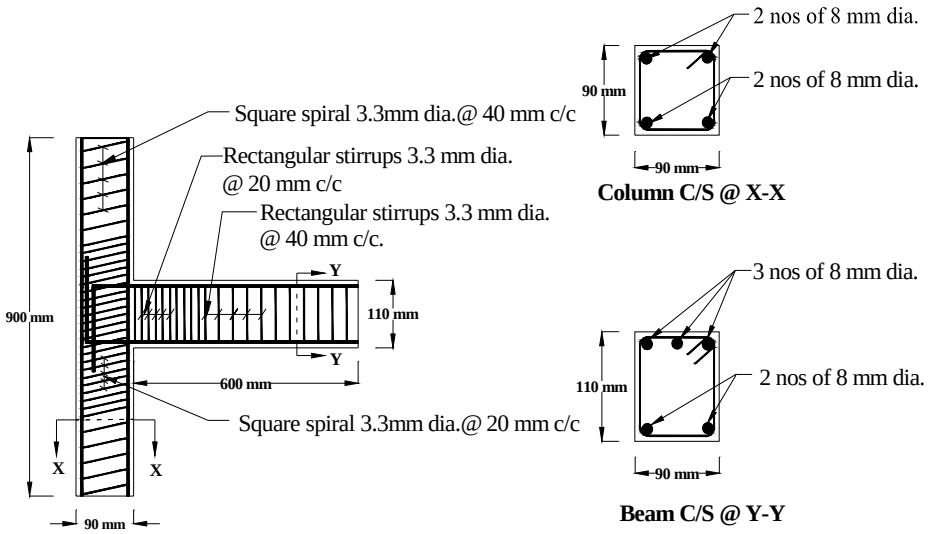

Figure 2. Reinforcement details of SS

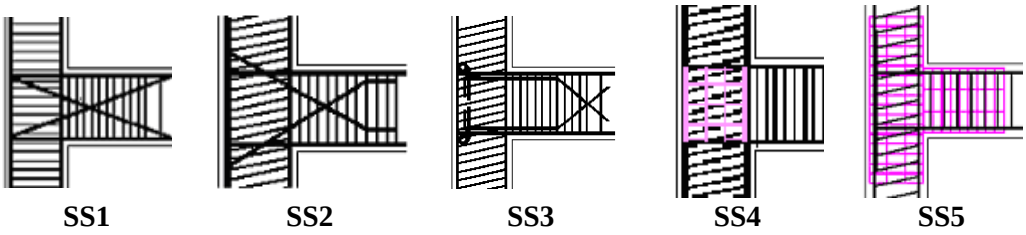

Figure 3. Various schemes of reinforcement detailing

Table 1: Percentage of reinforcement in test specimens

Description	SS, SS1	SS2	SS3	SS4	SS
%of A_{s1b}	1.52	2.54 (up to 2D) 1.52 (beyond 2D)	2.54 (up to 2D) 1.52 (beyond 2D)	1.52	1.64 (up to 2D) 1.52 (beyond 2D)
%of A_{s2b}	1.02	2.03 (up to 2D) 1.02 (beyond 2D)	2.03 (up to 2D) 1.02 (beyond 2D)	1.02	1.13
% of A_{sc}	1.24	3.72 (up to170mm from beam top and beam bottom) 1.24 (beyond 170mm)	1.24	2.48	2.62
%of A_{sj}	1.16	1.16	1.16	1.57	1.11

where

A_{s1b} - Area of longitudinal reinforcement at top face of the beam
A_{s2b} - Area of longitudinal reinforcement at bottom face of the beam
A_{sc} - Area of longitudinal reinforcement at interior face of column
A_{sj} - Area of transverse reinforcement in joint region

2.2 Materials

Concrete was made with 43 Grade Ramco Cement, river sand and 6mm crushed aggregate. The quantities of materials per cubic meter of concrete were as follows

Cement = 412 kg
Water/cement ratio = 0.5
Water = 206 litre
Coarse Aggregate = 953.09 kg
Fine Aggregate = 719 kg

The 28th day cube compressive strength of all the specimens was 37.52Mpa

2.3 Test setup and loading

The specimens were tested with the column portion vertical in a 100 ton reinforced concrete reaction frame as shown in Figure 4. No axial compression was applied to the columns in order to evaluate a worst-case scenario for the joint core. The column ends were attached to pivot assemblies at both ends to provide hinge conditions to simulate point of inflexion at both sides of the column. Screw jacks were placed on top and bottom of beam by which displacement controlled loading was applied. Proving rings were attached to screw jacks which were used to measure the load applied to the beam end. The deflections and rotations of beam were measured by dial gauges. The strain was measured from steel rods which were welded to beam reinforcement by Whittemore Strain Gauge.

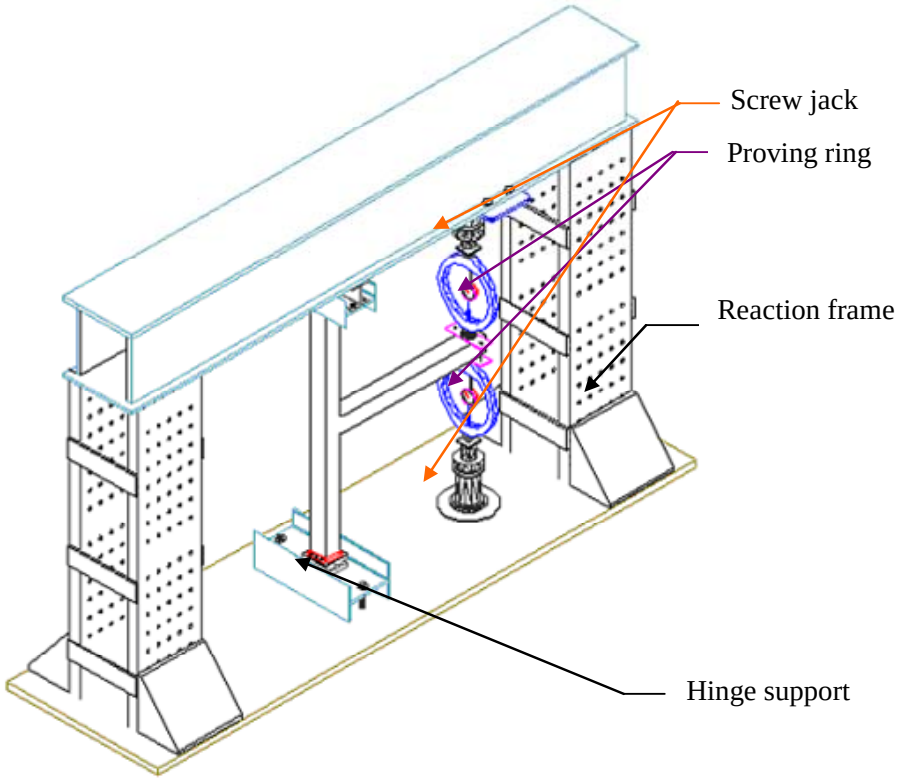

Figure 4. Schematic diagram of test setup

The loading programme consisted of a simple history of reversed symmetric displacement of increasing amplitudes 5mm, 10mm, 15mm, 30mm and 45mm as shown in Figure 5. The loading in positive direction of first 5 mm displacement cycle was numbered as “1” and the numbering was continued up to the last 45 mm displacement cycle. The two cycles of 5 mm displacement were named as “1A”, “1B” and that of 10 mm displacement as “2A”, “2B” and so on.

During each cycle, the loading was temporarily stopped at Y/4 mm displacement intervals where ‘Y’ is the peak displacement value for a cycle so as to enable the readings from dial gauges and proving ring to be noted. The readings from strain points were noted only at peak displacement values.

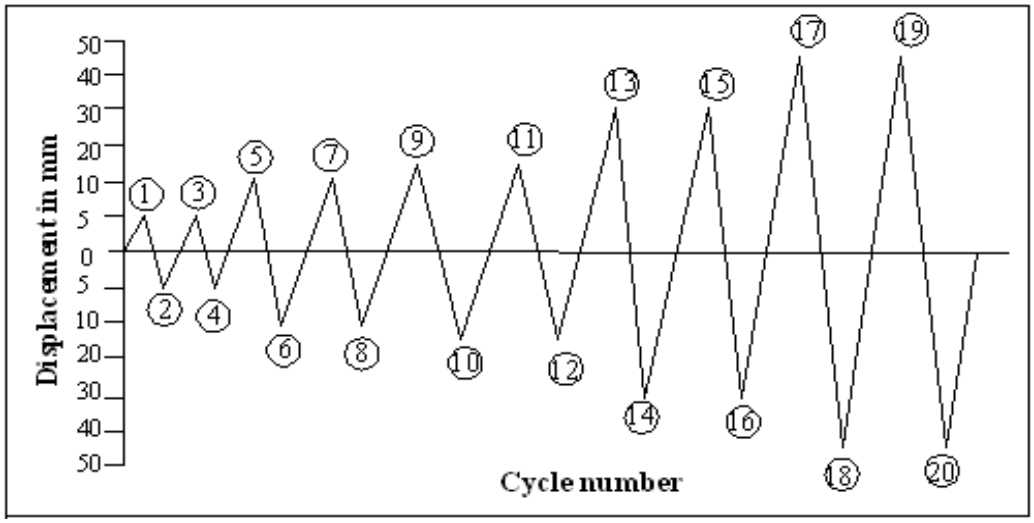

Figure 5. Cyclic displacement loading history applied on the test specimens

3. RESULTS AND DISCUSSION

3.1 Hysteresis behaviour

From the lateral load-displacement hysteresis loops (Figures 6a to 6f) of specimens, it is observed that SS, SS2, SS4 and SS5 possessed spindle shaped curves without pinching showing SS2 with the highest load carrying capacity of 15.6kN. There was steady increase in load with every increased displacement which continued even after 30mm displacement cycles. This proved that all these specimens had not failed till the 45mm displacement cycle. SS1 and SS3 experienced severe pinching and failed due to slippage of beam and column bars passing through the joint and joint shear deterioration respectively. The experimental maximum load of SS2 was greater than the experimental maximum load of SS, SS1, SS3, SS4 and SS5 by 22%, 30%, 33%, 19% and 18% respectively.

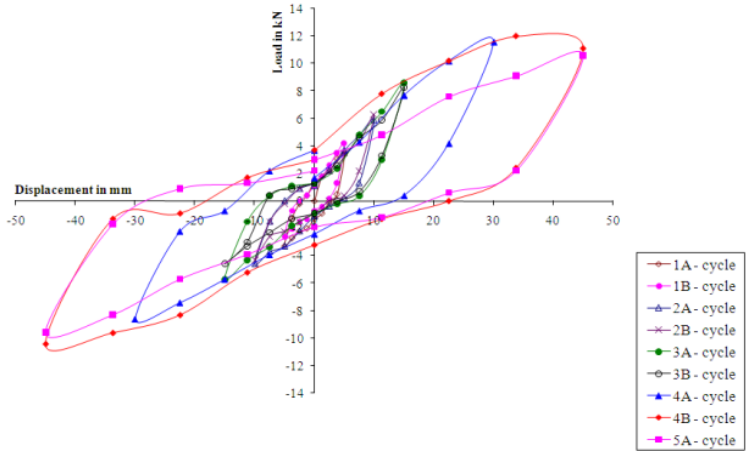

(a) SS

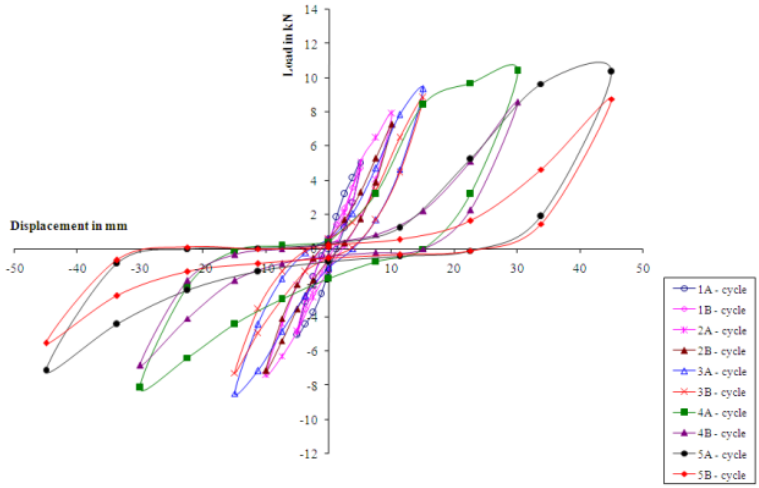

(b) SS1

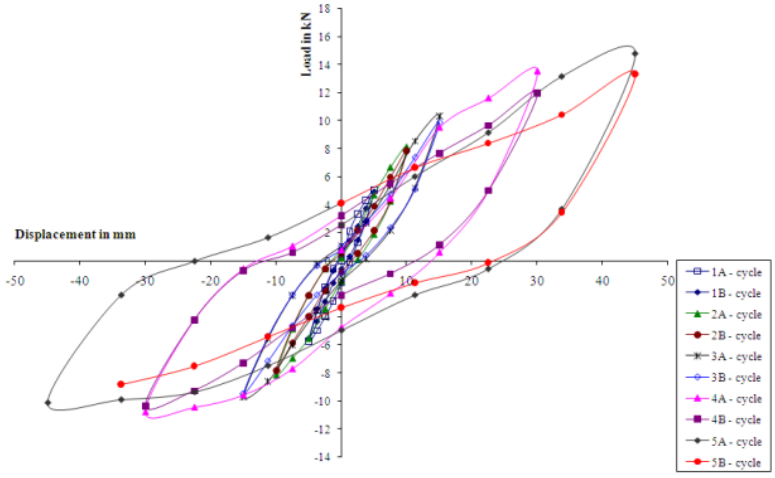

(c) SS2

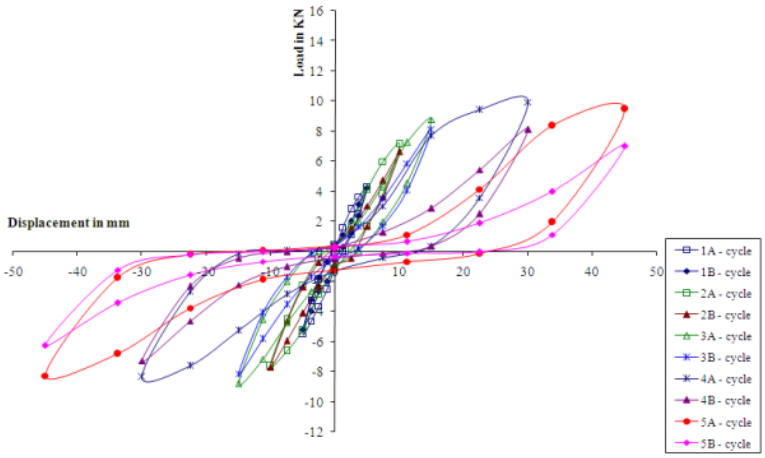

(d) SS3

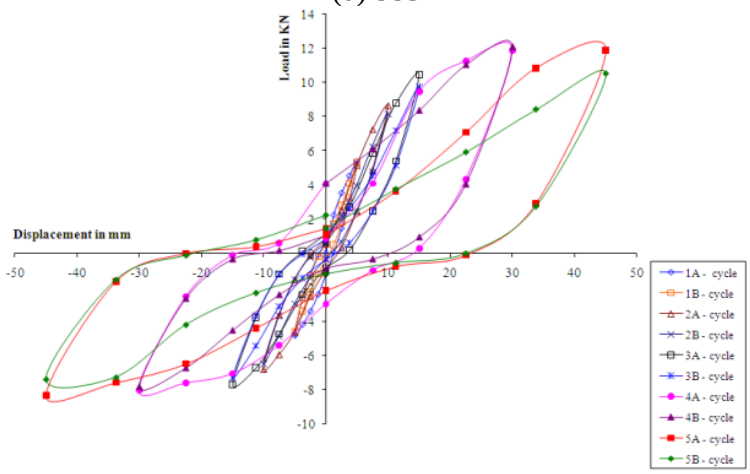

(e) SS4

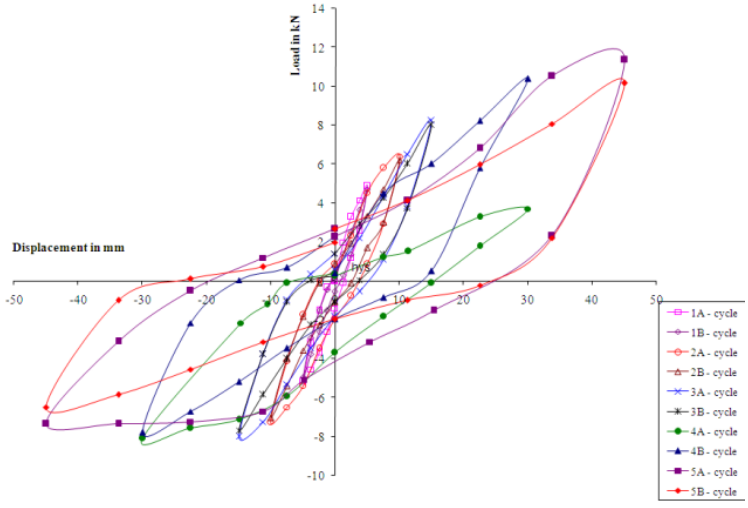

(f) SS5

Figure 6. Lateral load-displacement hysteresis loop

3.2 Load ratio

To examine the ability of each specimen to maintain its yield load-carrying capacity in the post elastic range, load ratio was calculated which is defined by Alameddine and Ehsani [9] as ratio between the average maximum load obtained during each cycle and the yield load of the specimen.

Table 2: Comparison of load ratio

Average of positive and negative displacement cycles	SS	SS1	SS2	SS3	SS4	SS5
5	1.05	1.08	1.35	1.37	1.09	1.1
10	1.77	1.68	2.03	2.11	1.64	1.53
15	2.23	1.99	2.5	2.46	1.92	1.78
30	3.03	2.21	3.04	2.68	2.12	2.04
45	3.05	2.2	3.12	2.65	2.14	2.11

The load ratio of SS2 was greater than the load ratio of SS, SS1, SS3, SS4 and SS5 by 2%, 42%, 18%, 46%, and 48% respectively (Table 2). The highest post-yield strength of SS2 was attributed to the combined effect of primary confinement with four additional bars of the specimens from column to beam which acted as additional flexure and shear reinforcement in the beam.

3.3 Stiffness

The percent of initial stiffness at the end of 45mm displacement cycle is presented in Figure 7. It is observed that SS2 retained the highest percentage of 31% of initial stiffness at the end of 45mm displacement cycle followed by SS, SS5, SS4, SS1 and SS3. The stiffness of SS, SS5, SS4, SS1 and SS3 after 45 mm displacement cycle was 30%, 24%, 23%, 22% and 21% respectively of their initial stiffness.

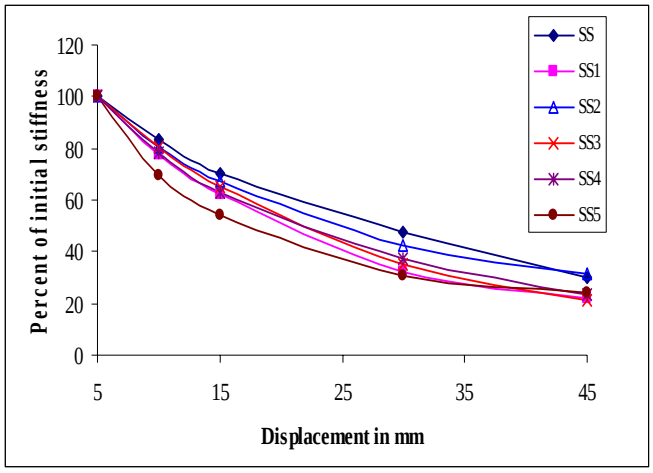

Figure 7. Percent of initial stiffness versus displacement curves

3.4 Energy dissipation

The effectiveness of any detailing scheme is in the amount of energy dissipated by the structural component provided with such a detailing scheme [1]. The energy dissipated during a particular loading cycle is computed as the area enclosed within the load versus displacement curve, starting and ending with a zero displacement [9].

From the cumulative energy versus displacement curves of specimens with square spiral confinement plotted in Figure 8, it is seen that the specimen SS2 had the highest value of E_t of 1231.03 kNmm. E_t of SS2 was greater than E_t of SS by 9%and that of SS4 and SS5 by 25% each. The total energy dissipated by SS2 was greater than E_t of SS1 and SS3 by an equal amount of 49%.

3.5 Beam rotation

The beam rotations were measured to identify the location of plastic hinge in the beam [9]. If the beam rotation at a distance of 2D was larger than beam rotation at D, it indicates the development of plastic hinge away from the column face. From Table 3 it is observed that SS2 had the lowest beam rotation of 0.056 radian at a distance of D. It is also observed that SS2 had its beam rotation over a distance of 2D greater than that of D from the face of column. θ_{2D} of SS2 was greater than its θ_D at 45 mm displacement by 28%.

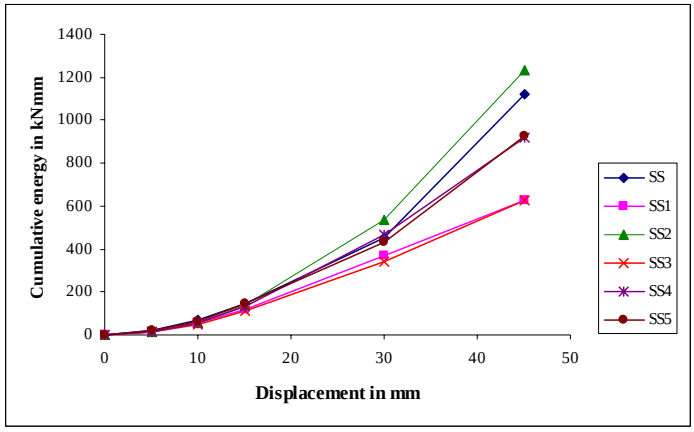

Figure 8. Cumulative energy versus displacement curves of SS series specimens

Table 3: Beam rotation of test specimens at distances of D and 2D at 45 mm displacement

Specimen	Beam rotation at a distance of D in radian	Beam rotation at a distance of 2D in radian
SS	0.207	0.115
SS1	0.092	0.082
SS2	0.056	0.077
SS3	0.085	0.068
SS4	0.09	0.083
SS5	0.091	0.087

In SS1 and SS3, joint region was subjected to excessive shear deformation and most of the inelastic actions were concentrated in the joint region and in the beam region adjacent to the joint region. Hence the rotation was higher at a distance of D in beam than the rotation at a distance of 2D. The joint reinforcement in SS, SS4 and SS5 was adequate to prevent joint shear failure but the plastic hinge was concentrated only in the beam region adjacent to column face. Hence these specimens had their beam rotation at a distance of D higher than the beam rotation at distance of 2D.

3.6 Strain behaviour

The strain values (Figure 9a) in beam top and bottom bar at face of column indicate that the specimens SS, SS2, SS4 and SS5 had cyclic tension and compression without slippage and yielded as the higher displacement cycles were imposed except SS1 and SS3. The beam top bars of SS1 and SS3 showed slippage after second -30mm (cycle number 16) and first +45 mm displacement (cycle number 17) respectively. The beam bottom bar (Figure 9b) of SS1 and SS3 showed reversal of direction in strain at second +5 mm displacement (cycle number 3) and first -10 mm (cycle number 6) respectively. Because there is no continuation of such tendency in the subsequent cycles, this indicates localized slip.

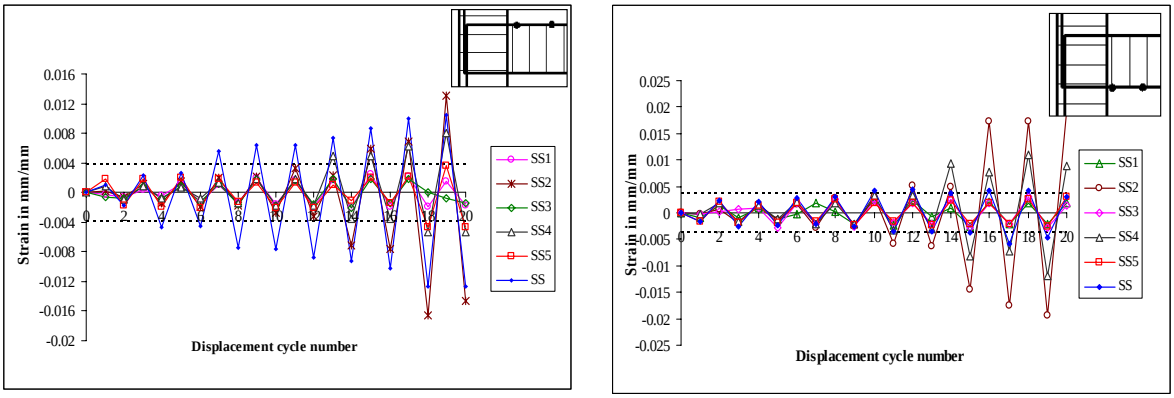

(a) Top bar (b) Bottom bar

Figure 9. Comparison of strain

3.7 Crack pattern

The crack pattern and location provide a first hand insight of the behaviour of the specimen. SS, SS4 and SS5 (Figure 10a, 10e and 10f) experienced minor damage in joint region due to shear cracks with only the domination of plastic hinge at the interface region. From Figure 10 b and 10d, it may be concluded that SS1 failed due to slippage of column and beam bars and SS3 failed only due to joint shear. SS2 (Figure 10b) experienced hairline 'X' shaped cracks in the joint region and full depth cracks in beam region approximately at a distance of 1.5D from the face of column. This confirmed that plastic hinge formed in the beam approximately at the location where the additional inclined bars were curtailed.

(a) SS

(b) SS1

(c) SS2

(d) SS3

(e) SS4

(f) SS5

Figure 10. Crack pattern

4. CONCLUSIONS

The following conclusions were reached from the present investigation:

a) Spindle-shaped hysteresis loops and better load carrying capacities were observed in

SS, SS2, SS4 and SS5. SS2 has the highest experimental maximum load of 15.6 kN. SS1 and SS3 experienced severe pinching in the hysteresis loops due to their low strength and stiffness.

b) The percent of initial stiffness retained at 45mm displacement of SS, SS2, SS4 and SS5 was higher than SS1 and SS3. SS2 retained the highest percent (31%) of initial stiffness among all the specimens.
c) SS2 dissipated the highest value of total energy of 1231 kNmm among all the specimens tested. SS1 and SS3 dissipated lower values of total energy at 45mm displacement compared to SS, SS2, SS4 and SS5.
d) SS2 only had its beam rotation at a distance of 2D greater than the beam rotation at distance of D confirming the relocation of plastic hinge. SS, SS2, SS4 and SS5 had higher beam rotation at a distance of D than the beam rotation at a distance of 2D.
e) The plastic hinge formed in SS, SS4 and SS5 at the beam-column interface whereas in SS2 it was at a distance of 1.5D from the face of column. SS1 and SS3 experienced severe joint shear deterioration due to which the specimens failed.
f) The beam main bars of SS, SS2, SS4 and SS5 possessed better anchorage with reduced bond deterioration. The beam bars in SS1 and SS3 experienced severe bond deterioration resulting in slip of the bars with the surrounding concrete.

REFERENCES

1. Murty CVR, Rai DC, Bajpai KK, Jain SK. Effectiveness of reinforcement details in exterior reinforced concrete beam-column joints for earthquake resistance, *ACI Structural Journal*, **100**(2003) 149-56.
2. Hanson NW, Connor HW. Seismic resistance of reinforced concrete beam-column joints, *Journal of the Structural Division, ASCE*, ST5, **93** (1967) 533-60.
3. Ehsani MR, Wight JK. Exterior reinforced concrete beam-to-column connections subjected to earthquake-type loading, *ACI Structural Journal*, **82**(1985) 492-99.
4. Tsonos AG, Tegos IA, Penelis GGr. Seismic resistance of type 2 exterior beam-column joints reinforced with inclined bars, *ACI Structural Journal*, **89**(1992) 3-12.
5. Kumar SRS, Raju BV, Rajaram GSBVS. Hysteretic behaviour of lightly reinforced concrete exterior beam-to-column joint sub-assemblages, *Journal of Structural Engineering, ASCE*, **29**(2002) 31-7.
6. IS 456: 2000, Indian Standard Plain and Reinforced Concrete Code of Practice.
7. IS 1893 (Part 1): 2002, Indian Standard Criteria for Earthquake Resistant Design of Structures, Part-1 General Provisions and Buildings.
8. IS 13920: 1993, Indian Standard Ductile Detailing of Reinforced Concrete Structures Subjected to Seismic Forces-Code of Practice.
9. Alameddine F, Ehsani MR. High strength RC connections subjected to inelastic cyclic loading, *Journal of Structural Engineering, ASCE*, **117**(1991) 829-50.